2009

Analysis of the tip roundness effects on the micro- and macroindentation response of elastic-plastic materials

JOURNAL OF MATERIALS RESEARCH, v.24, n.3, p.1037-1044, 2009
http://producao.usp.br/handle/BDPI/14683

Analysis of the tip roundness effects on the micro- and macroindentation response of elastic–plastic materials

Sara Aida Rodríguez Pulecio,[a] María Cristina Moré Farias, and Roberto Martins Souza
Surface Phenomena Laboratory, Department of Mechanical Engineering, University of São Paulo, 05508-900 São Paulo - SP. Brazil

(Received 1 August 2008; accepted 6 November 2008)

In this work, the effects of indenter tip roundness on the load–depth indentation curves were analyzed using finite element modeling. The tip roundness level was studied based on the ratio between tip radius and maximum penetration depth (R/h_{max}), which varied from 0.02 to 1. The proportional curvature constant (C), the exponent of depth during loading (α), the initial unloading slope (S), the correction factor (β), the level of piling-up or sinking-in (h_c/h_{max}), and the ratio h_{max}/h_f are shown to be strongly influenced by the ratio R/h_{max}. The hardness (H) was found to be independent of R/h_{max} in the range studied. The Oliver and Pharr method was successful in following the variation of h_c/h_{max} with the ratio R/h_{max} through the variation of S with the ratio R/h_{max}. However, this work confirmed the differences between the hardness values calculated using the Oliver–Pharr method and those obtained directly from finite element calculations; differences which derive from the error in area calculation that occurs when given combinations of indented material properties are present. The ratio of plastic work to total work (W_p/W_t) was found to be independent of the ratio R/h_{max}, which demonstrates that the methods for the calculation of mechanical properties based on the indentation energy are potentially not susceptible to errors caused by tip roundness.

I. INTRODUCTION

The instrumented indentation technique (IIT), frequently called nanoindentation, is today one of the most commonly used techniques to measure mechanical properties of films and small volumes. The IIT uses high-resolution instrumentation for control and measurement of loads and depths of indenter penetration, when it is applied to and withdrawn from the studied material, in a cycle of loading and unloading. These tests are usually conducted with indenters that have deviations from the ideal geometry, because of manufacturing tolerances and wearing off due to excessive use. Therefore, many works have focused on the calibration of area functions to determine the precise geometry of the indenters.[1–3]

These geometrical deviations seriously affect the values of hardness when measurements are conducted at penetration depths with magnitude similar to the indenter radius.[4–6] In these cases, the changes in the shape of the loading curve can also be confused with those caused by the material work hardening,[7] which leads to errors in the calculation of the work-hardening coefficient. Furthermore, significant changes on the correction factor β, used to adjust Sneddon's equations,[8–12] have been recently observed due to indenter tip roundness.

Therefore, indenter tip radius may affect not only hardness and elastic modulus calculations, but also other variables of the indentation test; which are used in different algorithms for the calculation of mechanical properties.[13–16]

One possible way to study the effect of indenter tip roundness is based on the ratio R/h_{max}. In the case of conical indenters with semiangle equal to 70.3°, significant deviations in the load–penetration curves,[17] hardness,[4,6] and relationship between plastic zone radius and maximum depth[18] are expected when the ratio R/h_{max} is larger than one. Furthermore, the indenter tip radius effect in the loading stage can be ignored for ratios $R/h_{max} \ll 0.5$.[17,18] Despite the results published so far, some questions still remain regarding how small the indenter tip roundness has to be to be ignored, so that one may differentiate this effect from others that also affect indentation data.

This work presents a study about the effect of indenter tip roundness on the indentation variables for a given set of indenter radii and tested material properties, as well as for ratio R/h_{max} values lower than 1.

II. INDENTATION VARIABLES

Figure 1 shows a typical curve of load as a function of penetration depth (P–h), obtained during instrumented

[a]Address all correspondence to this author.
e-mail: sara.pulecio@poli.usp.br
DOI: 10.1557/JMR.2009.0078

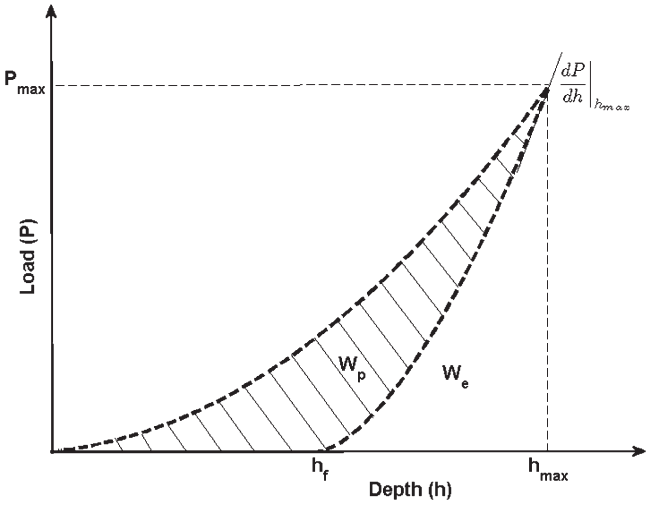

FIG. 1. Schematic representation of a typical load–displacement response of an elastic–plastic material to instrumented sharp indentation.

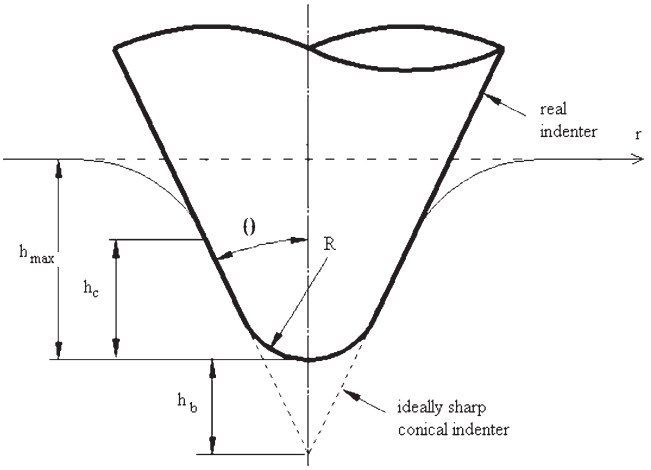

FIG. 2. Representation of an ideally sharped conical indenter and the same indenter with a spherical tip.

indentation tests. The initial unloading slope (S) is defined as dP/dh at the maximum load, in which P_{max} is the maximum load obtained in the test, h_{max} is the maximum indentation depth, h_f is the residual indentation depth after complete unloading, $W_t = W_e + W_p$ is the work done by load P during the loading cycle, W_p is the stored (plastic) work after the complete unloading, and W_e is the area under the unloading curve, which corresponds to the elastic work recovery of the material.

During the loading stage, the material response generally follows this relation[1]:

$$P_l = Ch^{\alpha} \quad , \tag{1}$$

in which exponent α is equal to 2 for a conical indenter with perfect shape (no tip roundness), and 3/2 for spherical indenters. C is a coefficient that indicates the curvature of the P–h loading curve.

During unloading, the P–h curve follows this relation[1]:

$$P_u = K(h_{max} - h_f)^m \quad , \tag{2}$$

in which K is the curvature of the unload curve and m is the exponent of the curve.

Hardness (H) is defined [Eq. (3)] as the maximum indentation load (P_{max}) divided by the contact area (A_c), which can be calculated based on Eq. (4), considering a conical indenter with semiangle equal to 70.3°.

$$H = \frac{P_{max}}{A_c} \quad , \tag{3}$$

$$A_c = 24.5 \cdot (h_c + h_b)^2 \quad , \tag{4}$$

$$h_b = R\left(\frac{1}{\sin(\theta)} - 1\right) \quad . \tag{5}$$

In Eq. (4), h_b is a measure of tip roundness and can be estimated through Eq. (5), in which θ is the half-angle of the cone (Fig. 2).

The response of the indented material is commonly considered as a function of (i) depth of penetration (h); (ii) mechanical properties of the material and the indenter, namely Young's modulus (E), initial yield stress (Y), strain-hardening exponent (n), and Poisson's coefficient (ν); (iii) geometrical parameters of the indenter, mainly tip radius (R) and semiapex angle (θ); and (iv) friction coefficient in the indenter-specimen contact (μ), and level of residual stresses in the specimen.[11,15,19,20]

The Young's modulus and the Poisson's ratio of the materials in the systems can be joined in one parameter: the reduced Young's modulus (E_r), which may be obtained as indicated in Eq. (6), in which E_i and ν_i are the Young's modulus and Poisson's ratio of the indenter, respectively.

$$\frac{1}{E_r} = \frac{(1-\nu^2)}{E} + \frac{\left(1-\nu_i^2\right)}{E_i} \quad . \tag{6}$$

Using the information from the instrumented indentation test, it is also possible to calculate the elastic modulus, using Eq. (7), in which β is a correction factor.

$$E_r = \frac{\sqrt{\pi}}{2\beta}\frac{S}{\sqrt{A_c}} \quad . \tag{7}$$

Equation (7) originated from Sneddon's equation[21] for axisymmetric indenters. In the form presented by Oliver and Pharr,[1] the factor β is equal to 1; yet, if the indenter is not symmetric, as the pyramidal ones, Eq. (7) should have a correction factor different from 1 and dependent on both indenter geometry and Poisson's coefficient.[22,23] Other works[8–12] found dependence of β in relation to the indentation size and, consequently, in relation to the indenter tip defects.

III. FINITE ELEMENT ANALYSIS

A finite element analysis, using the commercial software ABAQUS (Providence, R1), was carried out to simulate the indentation response of elastic–plastic solids. The indenter was a rigid two-dimensional (2D) cone with apex angle equal to 70.3°, so that the ratio projected area/depth of the cone was the same as that of the Berkovich or Vickers pyramidal indenters.[13,14,24,25] It is worth mentioning that although the P–h curves are similar, significant differences on all indentation parameters are expected between the conical and pyramidal cases.[16,26]

The material tested was represented by a 2D mesh using 37,282 four-noded, axisymmetric type CAX4R elements. The mesh close to the contact was refined to improve the accuracy and convergence of the analysis, and the mesh became gradually coarser when moving away from the initial contact region. The element located at the initial point of contact was a square with sides equal to 30 nm in length. In addition, in each finite element simulation the minimum number of elements in contact with the indenter at maximum load was 66. Regarding the boundary conditions, the nodes at the axis of symmetry were allowed to move only vertically, and the nodes at the bottom were fixed. In all finite element computations, the contact has been modeled considering two surfaces with isotropic friction; contact that follows the model of Coulomb,[27] with friction coefficient equal to 0.15.[25] The specimen was modeled as a homogeneous and isotropic solid. The elastic and plastic behaviors of the indented material followed Hook's law and hardening power law, respectively, as indicated in Eq. (8). In all simulations, a large deformation formulation was considered.

$$\sigma = \begin{cases} E\epsilon \ \ for\, \sigma \le Y \\ K\epsilon^n \ \ for\, \sigma > Y \end{cases} \quad . \tag{8}$$

Using dimensional analysis, different authors have found that the material indentation response depends on the dimensionless variables Y/E, R/h, and n, which have physical meaning. Y/E and n are mechanical properties: Y/E is the strain from which the indented material deformation is no longer elastic, and n is the strain-hardening exponent of the indented material.[13–16,19] The parameter R/h is a geometric factor that relates the indenter deviation from a perfect shape, characterized by the indenter tip roundness and the depth of penetration.[4,10,17] These variables were used in this work, considering three levels for each one. The ratio Y/E was set equal to 0.001, 0.01, or 0.1; the strain-hardening exponent of the indented material n was set equal to 0, 0.25, or 0.5; and the ratio R/h_{max} was set equal to 0.02, 0.5, or 1. All possible combinations of these values of Y/E, R/h, and n were considered, totalizing 27 finite element simulations. In all cases, the simulations were conducted up to a maximum depth of 1 μm.

In this work, the values of the Poisson's ratio and Young's modulus of indented material, and the angle of the conical indenter were fixed, being equal to 0.3, 100 GPa, and 70.3°, respectively. Additionally, the indented material was considered free from residual stresses.

IV. RESULTS AND DISCUSSION

The loading steps of the P–h curves obtained in the finite element simulations were adjusted to Eq. (1), which provided the values of P_{max}, C, and α for each case.

Figure 3 presents the values of α calculated on the basis of the data from all simulations. As indicated in the figure, α tends to two when the ration R/h_{max} tends to zero, but diverges from two when the ration R/h_{max} increases. For each R/h_{max} value, variations lower than 0.8% in α were obtained due to differences in the mechanical properties.

A linear fit [Eq. (9)] was adjusted to all simulation data, which provided a correlation coefficient of 0.99 and an error of ±0.51%.

$$\alpha = 2.0035 - 0.176\frac{R}{h_{max}} \quad . \tag{9}$$

Therefore, assuming that α is mainly a function of R/h_{max}, this ratio can be experimentally determined. Once the equipment compliance has been carefully calculated,[28] fitting the load curve to Eq. (1), it provides the exponent α, which allows the calculation of R/h_{max} through Eq. (9).

Equation (9) should not be used for large R/h_{max}, because the expression was validated for R/h_{max} lower than 1.6. Besides, the use of this expression should occur only when the contact is predominantly conical; when the contact is spherical the value of α is 2/3.

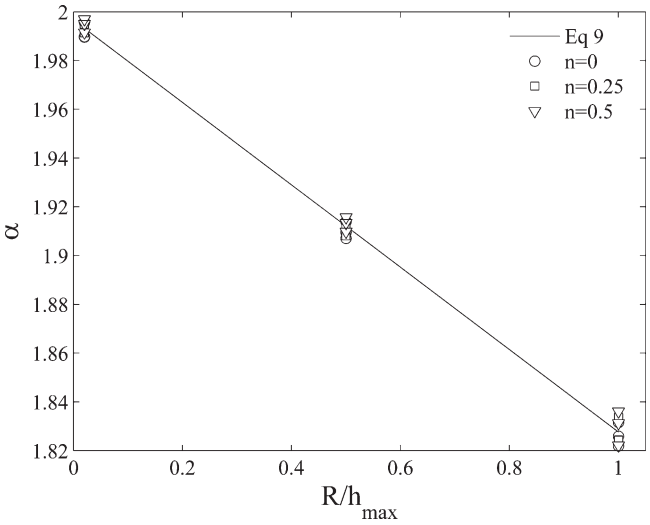

FIG. 3. Tip roundness effect on the exponent of loading curve α.

Figure 4 shows the changes of P_{max} with the ratio R/h_{max}, the ratio Y/E, and the hardening coefficient n. The variation of P_{max} with R/h_{max} is low and linear, and therefore consistent with data previously reported in the literature.[17] However, when the tip roundness effect is not considered, the variation caused by the ratio R/h_{max} can be confused with the effect of the hardening coefficient, because an increase in values of these two variables, n and R/h_{max}, produces an increase in the value of P_{max}. This type of confusion is more probable for larger values of the ratio Y/E. Figure 4 shows that for $Y/E = 0.1$ the variation in the value of P_{max}, caused by the increment of the ratio R/h_{max} from 0.02 to 0.5, is equivalent to the variation caused by an increase in the hardening coefficient from 0 to 0.5. The variations caused by the increase in the ratio R/h_{max} from 0.02 to 1 ranged from 11.06% to 13.34% for all mechanical property combinations simulated, with no apparent synergy between the tip roundness effect and mechanical property effects.

Besides the analysis of the effect of the ratio R/h_{max} on the indentation parameters computed from finite elements calculations, an analysis of the sensitivity of the estimated mechanical properties (from reverse algorithms) to variations in the indentation parameters (C, S, h_f, h_{max}) and its correlation with the tip radius effect can also be done based on the results taken from the literature.

In the case of a perfect indenter, for which a square dependence between the load and depth of the loading stage has been established, small variations in C value obtained from Eq. (1) would lead to significant errors in the plastic properties (Y, n) estimated by the reverse analysis proposed in Ref. 13. Because Figs. 3 and 4 show a significant influence of the R/h_{max} ratio in the loading curve parameters, it might be expected that significant errors would result in mechanical properties calculation if the radius effect is neglected.

All unload curves were fitted to Eq. (2) using 67% of the initial unloading data,[9,13] which provided the values of parameters K, m, and h_f. Figure 5 shows the variation of the initial unloading slope (S) considering ratio R/h_{max}, ratio Y/E and hardening coefficient n. For materials with ratio $Y/E = 0.1$, the variations caused by increasing the ratio R/h from 0.02 to 1 are of 6.07%, 2.2 times the variation caused by the change in the rate hardening of 0 to 0.5. However, the variation caused by the tip roundness can be confused with those caused by both ratio Y/E (for the smaller values of Y/E of 0.001 and 0.01) and hardening coefficient n. Although the influence of the ratio R/h on S values found in this work are around 6%, smaller variations (2% and 4%) in the unloading slope (S) can make inaccurate the calculation of mechanical properties using the not radius-dependent reverse algorithm proposed in Ref. 13, because large errors in the estimated values of the yield strength and strain-hardening coefficient were obtained. Thus, once the unloading slope (S) appears to be affected by the ratio R/h_{max}, as indicated in Fig. 5, it is plausible to state that the inclusion of the tip radius in such algorithm would reduce the error in the predicted plastic properties.

Figure 6 presents the results of variation of ratio h_c/h_{max}, which defines the level of piling-up or sinking-in,[30,31] with the values of R/h_{max}, Y/E, and n. In this case, in the ranges studied the tip roundness effect does not follow the trend observed for other variables. If the material is prone to the formation of piling-up ($h_c/h_{max} > 1$), the tip roundness effect provides a slight increase in the tendency for piling-up formation. Similarly, and in general, if the material is prone to the formation of sinking-in, the tip roundness effect provides a slight increase

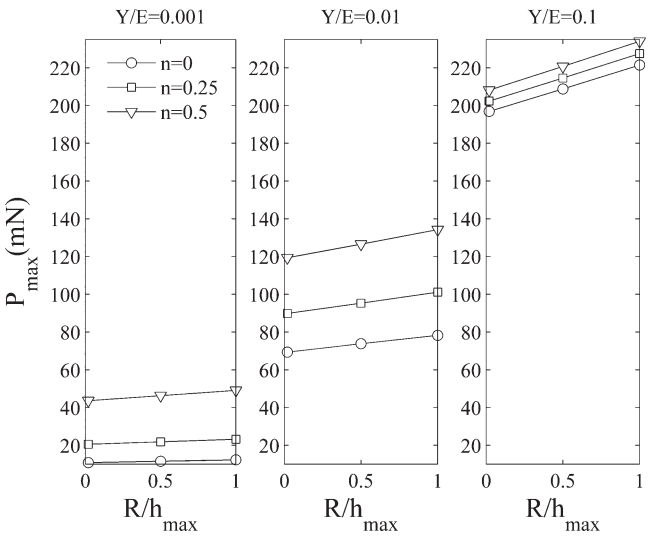

FIG. 4. Tip roundness effect on maximum load P_{max}.

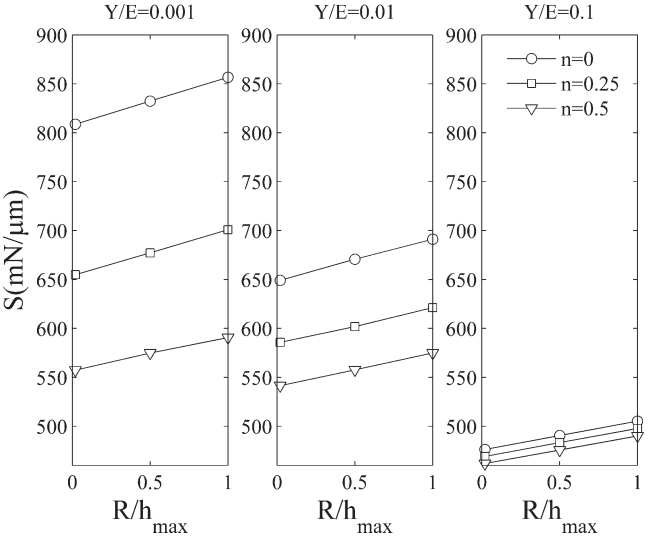

FIG. 5. Effect of indenter tip rounding on initial unloading slope (S).

in the tendency for sinking-in formation. The literature indicates an increase in the level of piling-up or sinking-in when moving from conical[30,31] to spherical[29] indentation. Thus, the increment on the level of piling-up or sinking-in with an increase on ratio R/h_{max} is consistent with these results.

Figure 7 shows a complex variation of β with ratio R/h_{max} for different mechanical property combinations. It indicates that the parameter β is not a constant, but changes along with materials properties and geometric defects of the indenter. The value of β has changed from 1.07 to 1.13 for the conditions studied in this work.

Contrary to the trend found in Ref. 10 of monotonic increase of β with ratio R/h_{max} for elastic materials, Fig. 7 shows that, for elastic–plastic materials, β may decrease or increase along with the increase on the ratio R/h_{max}, depending on ratio Y/E and on the strain-hardening exponent (n). Additional research is still required to further understand these variations on the value of β.

Throughout the range of mechanical properties studied in this work, the effect of tip roundness on the ratio W_p/W_t is small, less than 1.5% in all cases. This result shows that the methods for calculating mechanical properties based on the energy of the indentation (see Ref. 32) are potentially not susceptible to errors caused by this variable.

Figure 8 shows the variation on the ratio h_{max}/h_f with R/h_{max}, Y/E, and n. In these cases, the residual indentation depth h_f was taken directly from the end of the unload simulation curve and not from Eq. (2). The variation is low when the ratio Y/E is small, but increases for the highest values of Y/E and n, reaching 23.41% for $Y/E = 0.1$ and $n = 0.5$.

Variations in the ratio h_{max}/h_f smaller than 1% can invalidate the reverse algorithm proposed by Casals et al.[16] for the calculation of mechanical properties, in which the radius effect was neglected. Thus, the inaccuracy of this reverse algorithm can also be related with the fact that the ratio h_{max}/h_f is affected by the ratio R/h_{max}, including R/h_{max} values lower than 1, as indicated in Fig. 8.

The increase of ratio R/h_{max} decreases the differences between ratio h_f/h_{max} and ratio W_p/W_t, as presented in Fig. 9. The relation between ratio h_f/h_{max} and ratio W_p/W_t was presented in Ref. 13 for sharp indenters, as a way of obtaining ratio W_p/W_t using ratio h_f/h_{max}. The roundness effect presented in this work indicates that tip roundness may affect the calculation of mechanical properties if that relation is used,[13,16] especially if the material presents a markedly elastic behavior (small values of W_p/W_t).

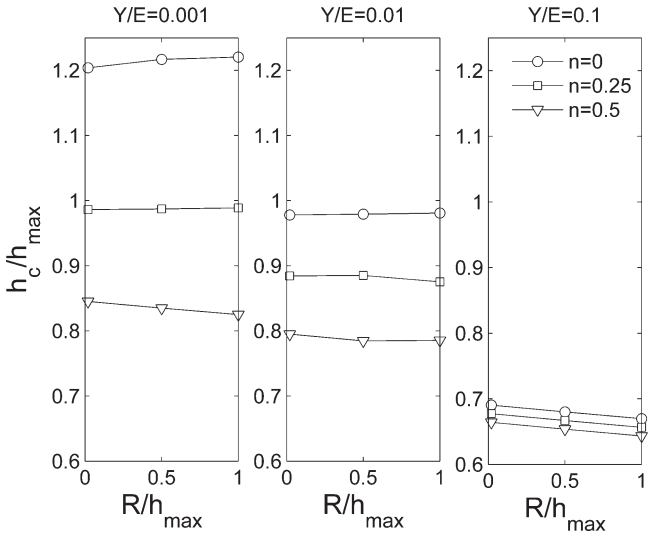

FIG. 6. Change in ratio h_c/h with ratio R/h.

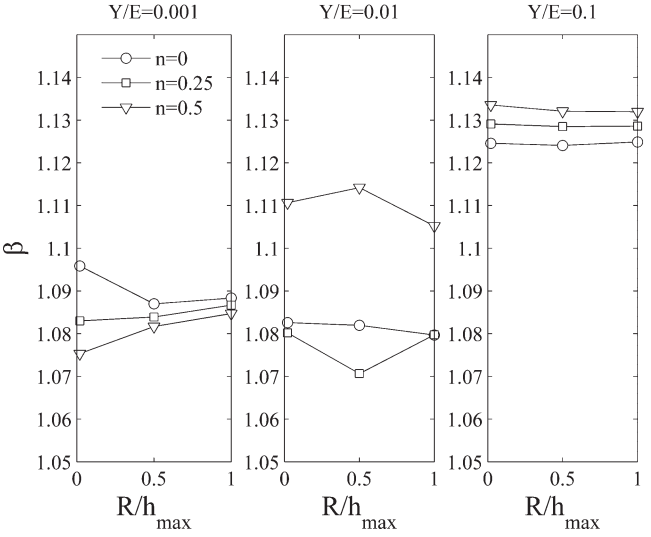

FIG. 7. Variation of parameter β with ratio R/h.

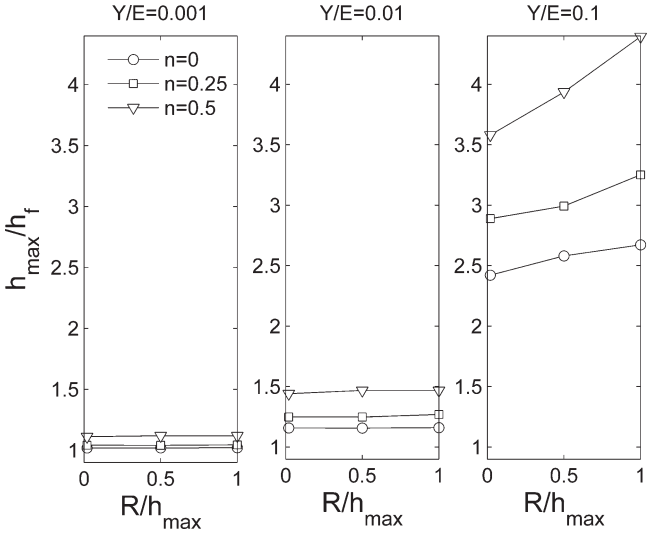

FIG. 8. Change in ratio h_{max}/h_f with ratio R/h.

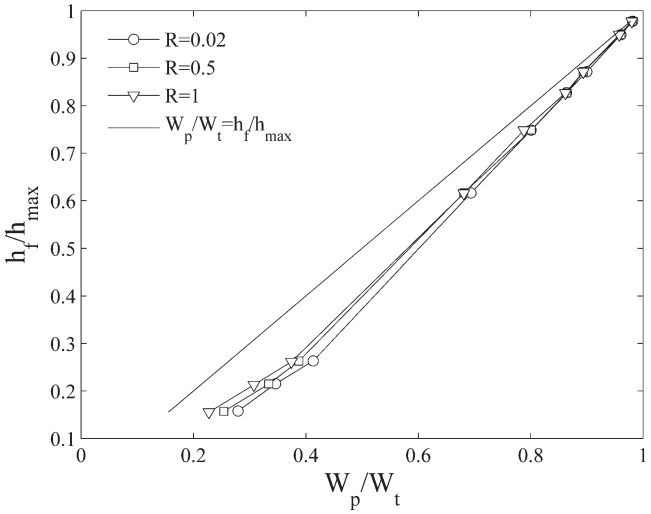

FIG. 9. Relation between ratio h_f/h_{max} and ratio W_p/W_t.

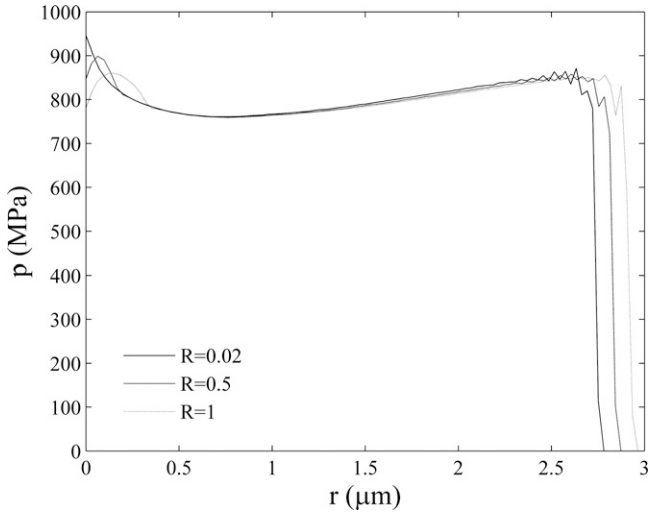

FIG. 10. Contact pressure distribution for a solid with ratio Y/E = 0.001, n = 0.25.

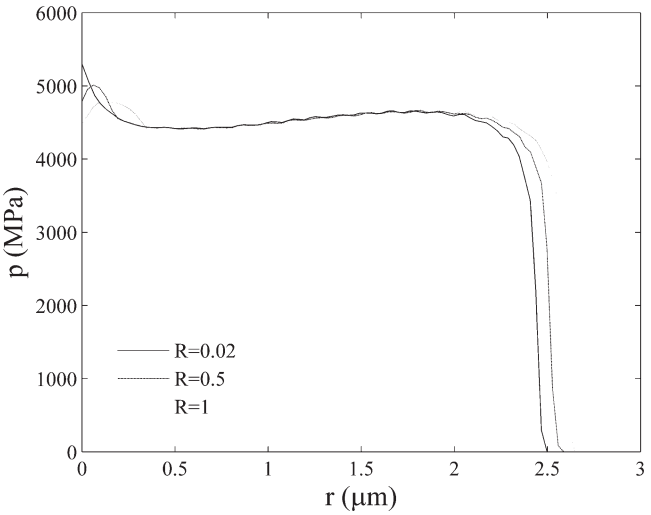

FIG. 11. Contact pressure distribution for a solid with ratio Y/E = 0.01, n = 0.25.

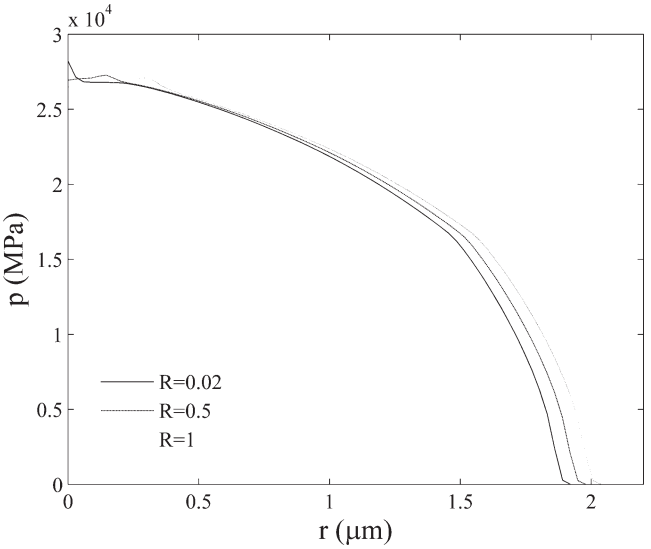

FIG. 12. Contact pressure distribution for a solid with ratio Y/E = 0.1, n = 0.25.

Unlike when $R/h >> 1$, where the hardness is considerably affected by the tip imperfection,[4,6] the variation on hardness is small when $R/h < 1$, between −1.17% and 1.91%. A better understanding of the role of tip roundness on the contact response of a strain-hardening solid can be achieved by comparing the contact pressures $p(r)$ calculated for different tip roundness values (Figs. 10–12). In this work, figures for n = 0 and n = 0.5 were not provided for the sake of brevity. As expected, the finite element simulations indicate that as Y/E and n increase, p gradually shifts to large stresses and the distribution of pressure tends to be less flat. Similar contact pressures were obtained in simulations considering the same specimen mechanical properties, with the exception of the indentation center (r = 0), on which a slight decrease in pressure was observed as the tip radius increased. Differences in contact pressure were also observed at the indentation border, where larger tip radii resulted in larger radii of contact, which explains the small variations observed in hardness. The decrease in contact pressure at r = 0 is produced both by the effect of the tip radii and the friction effect. Thus, one could expect an interaction between the effects caused by friction and tip roundness, which should be studied more deeply in the future.

The use of Eq. (10), proposed by Oliver and Pharr,[1] allows an alternative route for the calculation of contact depth h_c. Once h_c is determined through this route, Eqs. (3), (4), (6), and (7) allow the calculation of hardness and elastic modulus according to Oliver and Pharr method.

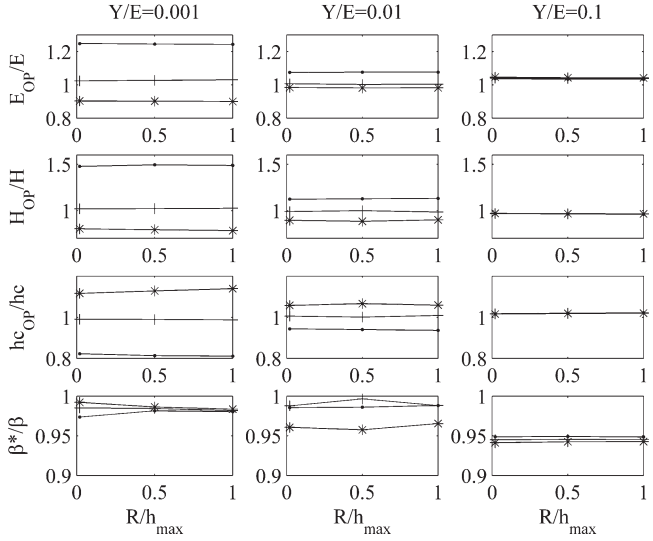

FIG. 13. Values of ratio obtained using the Oliver and Pharr procedure and those directly from finite element calculations for • $n = 0$, + $n = 0.25$, * $n = 0.5$.

$$h_c = h_{max} - \gamma \frac{P_{max}}{S} \quad , \qquad (10)$$

where γ is a geometrical parameter, dependent on the indenter geometry ($\gamma = 0.72$ for a conical indenter, $\gamma = 0.75$ for paraboloid of revolution, and $\gamma = 1$ for a flat punch[1]).

Figure 13 shows the ratios between quantities, E_{OP}/E, H_{OP}/H, h_{cOP}/h_c, and β^*/β, calculated according to the Oliver and Pharr method, and those obtained directly from finite element calculations (using $\gamma = 0.72$[1] and $\beta^* = 1.067$[33]). Equation (10) is successful in following the variation of h_c with the ratio R/h_{max} through the variation of S with the ratio R/h_{max}. The error on the calculation of hardness using the Oliver and Pharr method varied from −21.7629% to 49.22%, and, for the calculation of elastic modulus, from −9.09% to 27.07%. Figure 13 clearly indicates that ratios increase as ratio Y/E decreases. A comparison with data regarding piling-up or sinking-in formation (Fig. 6) indicates that the largest discrepancies occur with piling-up formation ($n = 0$ and $Y/E = 0.001$), which has already been reported in the literature.[30,31] However, Fig. 13 also indicates that different values may be obtained even when there is sinking-in formation.

V. CONCLUSIONS

The influence of indenter tip roundness on characteristics of the instrumented indentation curve was studied for conical indentations, considering a tip roundness level R/h_{max} smaller than one. Although the situation involving the range $R/h_{max} < 1$ is outside the range in which the tip roundness exerts the biggest influence on the indented variables ($R/h_{max} > 1$), this condition is still not entirely understood. Therefore, the objective of this work was to quantify tip roundness effects in the range where their effect is routinely considered negligible. Besides, it is important to mention that many researchers mainly work with indentation equipments where the load range goes from approximately 10 mN to 1 N (microindentation field), for which it is not usual to operate with R/h_{max} ratios larger than one.

Under these considerations, following are the main conclusions of this work. The proportional curvature constant (C), the exponent of the depth in the load relation (α), the initial unloading slope (S), the correction factor (β), the level of piling-up or sinking-in (h_c/h_{max}), and ratio h_{max}/h_f are strongly influenced by ratio R/h_{max}.

The hardness (H) was found to be independent, but when that is calculated using methods that consider neither effects such as piling-up nor tip roundness effects, it may be incurring in large errors.

The ratio of plastic work to total work (W_p/W_t) is not susceptible to errors induced by the variations in R/h_{max}, which points out energy-based methods as potential approaches for the calculation of mechanical properties.

Results have also indicated that maximum contact pressure increased as Y/E and n increased, and that contact pressure decreased at $r = 0$ when the tip ratio increased. The distributions of contact pressure have changed due to the effect of the tip radius. Differences were observed from $r = 0$ to the point where the spherical surface meets the conical surface. No changes in contact pressure were found from this point up to the region close to the indentation edge. However, at the edges, larger tip radii resulted in larger radii of contact, which explains the small variation in hardness as a function of the ratio R/h_{max}.

ACKNOWLEDGMENTS

This research was sponsored by The National Council for Scientific and Technological Development (CNPq) under Contract No. 141259/2007-8 and by The State of Sao Paulo Research Foundation (FAPESP).

REFERENCES

1. W.C. Oliver and G.M. Pharr: An improved technique for determining hardness and elastic modulus using load and sensing indentation experiments. *J. Mater. Res.* **7,** 1564 (1992).
2. J.M. Antunes, A. Cavaleiro, L.F. Menezes, M.I. Simões, and J.V. Fernandes: Ultra-microhardness testing procedure with Vickers indenter. *Surf. Coat. Technol.* **149,** 27 (2002).
3. M.R. VanLandingham, T.F. Juliano, and M.J. Hagon: Measuring tip shape for instrumented indentation using atomic force microscopy. *Meas. Sci. Technol.* **16,** 2173 (2005).
4. W. Chen, M. Li, T. Zhang, Y.T. Cheng, and C.M. Cheng: Influence of indenter tip roundness on hardness behavior in nanoindentation. *Mater. Sci. Eng. A*, **445–446,** 323 (2007).
5. D. Ma, C.W. Ong, and S.F. Wong: New relationship between Young's modulus and nonideally sharp indentation parameters. *J. Mater. Res.* **19**(7), 2144 (2004).

6. D. Ma, C.W. Ong, and T. Zhang: An improved energy method for determining Young's modulus by instrumented indentation using a Berkovich tip. *J. Mater. Res.* **23**(8), 2106 (2008).
7. K.D. Bouzakis, N. Michailidis, S. Hadjiyiannis, G. Skordaris, and G. Erkens: The effect of specimen roughness and indenter tip geometry on the determination accuracy of thin hard coatings stress–strain laws by nanoindentation. *Mater. Char.* **49,** 149 (2003).
8. J.M. Meza and E.J. Cruz: Tip roundness effect in mechanical properties measured by instrumented indentation. *Sci. Teach.* **36,** 613 (2007).
9. J.M. Antunes, L.F. Menezes, and J.V. Fernandes: Three-dimensional numerical simulation of Vickers indentation tests. *Int. J. Solids Struct.* **43,** 784 (2006).
10. J.M. Meza, F. Abbes, and M. Troyon: Penetration depth and tip radius dependence on the correction factor in nanoindentation measurements. *J. Mater. Res.* **23,** 725 (2008).
11. M. Troyon and L. Huang: Correction factor for contact area in nanoindentation measurements. *J. Mater. Res.* **20,** 610 (2005).
12. M. Troyon and S. Lafaye: About the importance of introducing a correction factor in the Sneddon relationship for nanoindentation measurements. *Philos. Mag.* **86,** 5299 (2006).
13. M. Dao, N. Chollacoop, K.J. Van Vliet, T.A. Venkatesh, and S. Suresh: Computational modeling of the forward and reverse problems in instrumented sharp indentation. *Acta Mater.* **49,** 3899 (2001).
14. J.L. Bucaille, S. Stauss, E. Felder, and J. Michler: Determination of plastic properties of metals by instrumented indentation using different sharp indenter. *Acta Mater.* **51,** 1663 (2003).
15. Y.T. Cheng and C.M. Cheng: Scaling, dimensional analysis, and indentation measurements. *Mater. Sci. Eng. R*, **44,** 91 (2004).
16. O. Casals and J. Alcalá: The duality in mechanical property extractions from Vickers and Berkovich instrumented indentation experiments. *Acta Mater.* **53,** 3545 (2005).
17. Y.T. Cheng and C.M. Cheng: Further analysis of indentation loading curves: Effects of tip rounding on mechanical property measurements. *J. Mater. Res.* **13,** 1059 (1998).
18. J. Chen and S.J. Bull: On the relationship between plastic zone radius and maximum depth during nanoindentation. *Surf. Coat. Technol.* **201,** 4289 (2006).
19. M. Mata and J. Alcalá: Mechanical property evaluation through sharp indentations in elastoplastic and fully plastic contact regimes. *J. Mater. Res.* **18**(7), 1705 (2003).
20. S. Suresh and A.E. Giannakopoulos: A new method for estimating residual stresses by instrumented sharp indentation. *Acta Mater.* **46,** 5755 (1998).
21. I.N. Sneddon: The relationship between load and penetration in the axisimetric Boussinesq problem for a punch of arbitrary profile. *Int. J. Eng. Sci.* **3,** 47 (1965).
22. R.B. King: Elastic analysis of some punch problems for a layered medium. *Int. J. Solids Struct.* **23,** 12 (1987) 1657.
23. J.C. Hay, A. Bolshakov, and G.M. Pharr: A critical examination of the fundamental relations used in the analysis of nanoindentation data. *J. Mater. Res.* **14**(6), 2296 (1999).
24. M. Li, W.M. Chen, N.G. Liang, and L.D. Wang: A numerical study of indentation using indenters of different geometry. *J. Mater. Res.* **19,** 73 (2004).
25. M. Mata and J. Alcalá: The role of friction on sharp indentation. *J. Mech. Phys. Solids* **52,** 145 (2004).
26. S. Swaddiwudhipong, J. Hua, K.K. Tho, and Z.S. Liu: Equivalency of Berkovich and conical load-indentation curves. *Modell. Simul. Mater. Sci. Eng.* **14,** 71 (2006).
27. Theory Manual 5.1-1, Abaqus, Version 6.7.
28. Y. Sun, S. Zheng, T. Bell, and J. Smith: Indenter tip radius and load frame compliance calibration using nanoindentation loading curves. *Philos. Mag. Lett.* **79,** 649 (1999).
29. B. Taljat and G.M. Pharr: Development of pile-up during spherical indentation of elastic–plastic solids. *Int. J. Solids Struct.* **41,** 3891 (2004).
30. A. Bolshakov and G.M. Pharr: Influences of pileup on the measurement of mechanical properties by load and depth-sensing indentation techniques. *J. Mater. Res.* **13,** 1049 (1998).
31. Y.T. Cheng and C.M. Cheng: Effects of "sinking in" and "piling up" on estimating the contact area under load in indentation. *Philos. Mag. Lett.* **78,** 115 (1998).
32. Y.T. Cheng and C.M. Cheng: Relationships between hardness, elastic modulus, and the work of indentation. *Appl. Phys. Lett.* **73,** 614 (1998).
33. W.C. Oliver and G.M. Pharr: Measurement of hardness and elastic modulus by instrumented indentation: Advances in understanding and refinements to methodology. *J. Mater. Res.* **19,** 3 (2004).